

Fluorescent Polystyrene–Fe₃O₄ Composite Nanospheres for In Vivo Imaging and Hyperthermia

By Donglu Shi,* Hoon Sung Cho, Yan Chen, Hong Xu, Hongchen Gu, Jie Lian, Wei Wang, Guokui Liu, Christopher Huth, Lumin Wang, Rodney C. Ewing, Sergei Budko, Giovanni M. Pauletti, and Zhongyun Dong

1 Although many research programs focus on surface-
2 functionalized quantum dots (QDs) as clinical tools to improve
3 medical diagnosis,^[1–14] the primary objective of these investiga-
4 tions has been imaging^[3,15] and only a limited number of studies
5 have explored other functionalities, including therapeutic treat-
6 ment using hyperthermia.^[16] The main purpose of this work is to
7 present a new strategy in biomedical nanotechnology that allows
8 simultaneous in vivo imaging and local therapy via hyperthermia.
9 This novel concept is based on a unique nanostructure consisting
10 of polystyrene nanospheres (PS NSs, ca. 100 nm in diameter)
11 fabricated with a narrow size distribution that are modified by
12 polyethylene oxide and that contain Fe₃O₄ nanoparticles
13 (5–10 nm) embedded in their matrices. QDs are
14 immobilized on the surfaces of these composite NSs, facilitating

1 fluorescent imaging. The Fe₃O₄ nanoparticles encapsulated in
2 the NSs respond to an external magnetic field by increasing the
3 temperature of the surrounding environment (i.e., hyperther-
4 mia), which can be used therapeutically to treat tumor cells
5 locally.^[16–18]

6 A schematic representation of the nanostructure design used
7 to produce magnetic NSs with surface-immobilized QDs
8 (QD–MNSs) is shown in Figure 1. The polyethylene-oxide-
9 modified PS–Fe₃O₄ NSs were synthesized by miniemulsion/
10 emulsion polymerization.^[19] Earlier research demonstrated that
11 particle size critically affects the superparamagnetic state of the
12 Fe₃O₄ nanoparticles and must be controlled for biomedical
13 applications.^[16] However, this work was limited to the use of
14 individual Fe₃O₄ nanoparticles in the range 5–10 nm because of:
1) bioincompatibility in medical diagnosis and treatment;
2) aggregation of small particles that precluded homogenous
dispersion in aqueous solutions; and 3) weak magnetic moments
leading to insufficient heating and a low driving force required for
magnetic manipulation.

The synthesis of a nanoscale spherical composite with a high
fraction of magnetite in its matrix can effectively maintain
considerable magnetic moments in an applied field for both
hyperthermia and magnetic guiding. Immobilization of QDs on
the surfaces of such MNSs introduces additional properties that
are desirable for localized cancer diagnosis. First, QDs on the NS
surfaces exhibit intense emission in the near-IR range of the
electromagnetic spectrum, which is ideal for deep-tissue
imaging.^[20] Second, introduction of multivalent, surface-
functionalized QDs allows coupling of unique tumor-targeting
ligands, such as antibodies, increasing selectivity of this
nanocomposite. Third, a high fraction of magnetite in the PS
composite exhibits much stronger magnetic moments which, in
contrast to individual Fe₃O₄ nanoparticles, significantly improves
magnetic manipulation and augments hyperthermia.

A drop of QD–MNS suspension was smeared on a glass slide
for microscopic evaluation using an Olympus BX51 equipped with
a fluorescence illumination module. Figure 2a shows a conven-
tional bright-field image of QD–MNS particles without fluores-
cence. The QD–MNS nanoparticles are clearly visible as individual
spherical units spread across the slide. Figure 2b shows the
fluorescence emission of the same area shown in Figure 2a after
excitation with light of wavelength, λ , = 540–580 nm and emission
at λ = 600–660 nm. Each particle exhibits intense red-light
emission against the dark background, suggesting effective
immobilization of QDs on the surfaces of the PS–MNSs. The
emission behavior of the QD–MNSs was further analyzed by laser
fluorescence spectrometry. The laser-excitation experiment was

[*] Prof. D. Shi, H. S. Cho, W. Wang, and C. Huth
Department of Chemical and Materials Engineering,
University of Cincinnati
493 Rhodes Hall, Cincinnati, OH 45221-0012 (USA)
E-mail: shid@email.uc.edu

Prof. Y. Chen
Key Laboratory of Nutrition and Metabolism, Institute for
Nutritional Sciences
Shanghai Institute for Biological Sciences, Chinese
Academy of Sciences
Shanghai 200031 (PR China)

Prof. H. Xu, Prof. H. Gu
Med - X Institute, Shanghai Jiao Tong University
Shanghai 200030 (PR China)

Prof. J. Lian, Prof. L. Wang, Prof. R. C. Ewing
Departments of Geological Sciences, Nuclear Engineering &
Radiological Sciences and
Materials Science & Engineering
University of Michigan
Ann Arbor, MI 48109 (USA)

Dr. G. Liu
Chemistry Division, Argonne National Laboratory
Argonne, IL 60439 (USA)

Dr. S. Budko
Ames Laboratory and Department of Physics and Astronomy
Iowa State University
Ames, IA 50011 (USA)

Prof. G. M. Pauletti
James L. Winkle College of Pharmacy, University of Cincinnati
Cincinnati, OH 45267 (USA)

Prof. G. Dong
Department of Internal Medicine, College of Medicine,
University of Cincinnati
Cincinnati, OH 45221 (USA)

DOI: 10.1002/adma.200803159

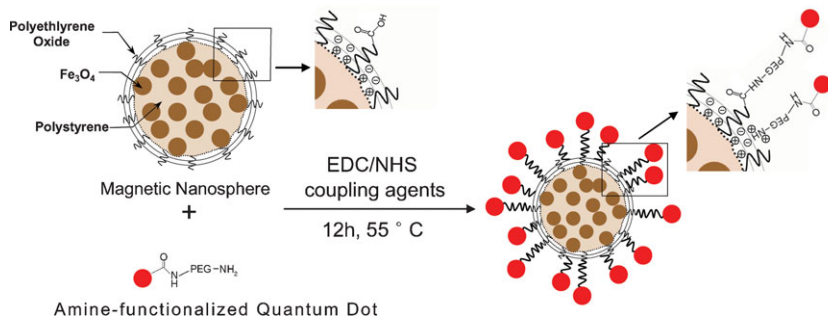


Figure 1. Schematic illustrating the surface-immobilized QDs on magnetic PS NSs. EDC: 1-ethyl-3-(3-dimethylaminopropyl) carbodiimide HCl; NHS: *N*-hydroxysuccinimide; PEG: polyethylene glycol. ■ We don't seem to have received the color cost confirmation forms. Please send us the completed forms. ■

1 completed at room temperature using a 355 nm neodymium-doped yttrium aluminum garnet (Nd:YAG) pulsed laser. The spectrum of the QDs associated with the MNS surface shows a broad peak around $\lambda = 770$ nm (Supporting Information, Fig. S1).

2 The surface structures of the QD-MNSs were characterized by transmission electron microscopy (TEM) using a JEOL 2010F microscope. TEM samples were prepared by dispersing the QD-MNSs directly on holey-carbon films supported on Cu grids. Figure 3a confirms the spherical shape of the PS-Fe₃O₄ composite particles in the bright-field with Fe₃O₄ nanoparticles (dark) embedded in the PS (light) matrix at a high concentration. High-resolution TEM imaging of the QD-MNSs (Fig. 3b) further supports the random distribution of surface-associated QDs on the composite NSs. The inset in Figure 3c is a Fourier-transformed image of a randomly selected nanoparticle, which can be indexed as ZnS. Figure 3b is the EDS spectrum, which is consistent with the chemical signals from CdSe/ZnS QDs. Combined, these data provide experimental evidence of successful immobilization of the commercial QDs onto the surfaces of the composite PS NSs.

3 To explore potential biological applications of this novel nanocomposite, fluorescence imaging of the QD-MNSs was performed in live mice. This study was approved by the Institutional Animal Use and Care Committee (IACUC) at the University of Cincinnati, in compliance with relevant state and federal regulations.

4 Using the Kodak Imaging station (Carestream Health, Inc., Rochester, NY; excitation: 725 nm, emission: 790 nm), *in vivo* fluorescence was monitored before and after intravenous injection of QD-MNSs (10 mg mL⁻¹ in phosphate buffered saline (PBS), 100 μ L of QD-MNS per animal) in nude mice via the tail vein.

5 Figure 4 shows the gray-scale fluorescence images from both control and QD-MNS-injected animals. The fluorescence images were acquired for 1 min. In the control, mouse autofluorescence was visible in certain ventral regions prior to QD-MNS administration (Fig. 4a). One day after injection, significant fluorescence attributed to the QD-MNSs was quantified in the anatomical region of the spleen (Fig. 4b).

6 The organs were harvested from the animals. As shown in insets of Figure 4a,b, *ex vivo* fluorescence images of the spleen indicate an accumulation of QD-MNSs in this organ of the treated mouse. No significant autofluorescence was measured in

7 the untreated control animal. To support these *in vivo* and *ex vivo* images with histological evidence, tissue was embedded in optimal cutting temperature compound (EMS, Hatfield, PA), and 10 μ m cryosections were prepared at -20 °C using an UltraPro 5000 cryostat (Vibratome Comp., Louis, MO). Microscopic evaluation of these sections in bright-field (Fig. 4c) and fluorescence (Fig. 4d) modes confirmed the accumulation of fluorescent QD-MNSs in nonsinusoidal mouse spleen with limited distribution into red pulp reticular meshwork. These data provide clear evidence that *in vivo* administration of QD-MNSs results in detectable fluorescence signals in a live animal. Current research efforts focus on

8 correlating surface properties of these novel nanocomposites with the biodistribution pattern after intravenous injection in mice using *in vivo* imaging.

9 Magnetic hysteresis and hyperthermia experiments were performed on the QD-MNSs. The hysteresis measurements

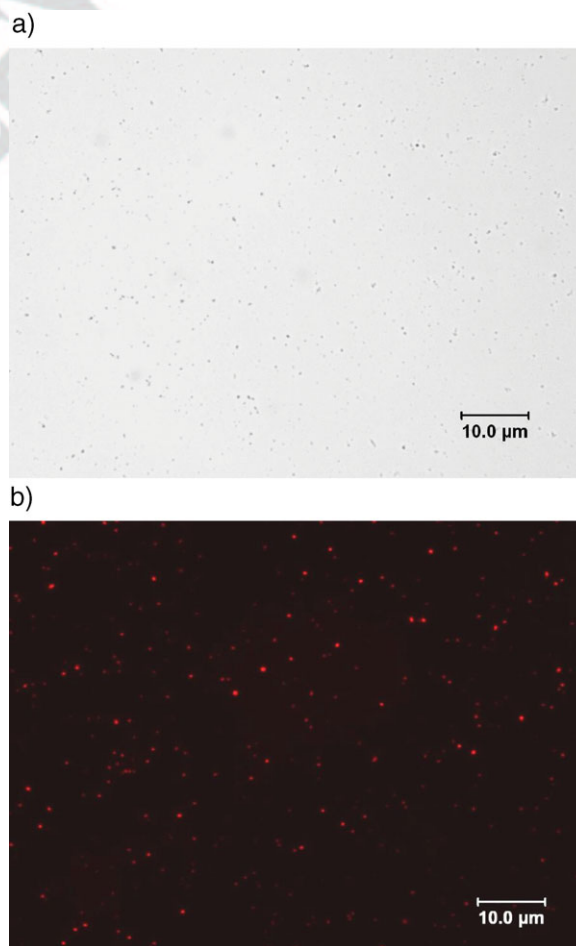


Figure 2. a) Bright-field optical image of dispersed MNSs with surface-immobilized Qdot 800 ITK amino (PEG) QDs. b) Fluorescence image of QD-MNSs obtained under excitation at 560 nm using a Texas Red emission filter set. ■ Thomson: Please add panel labels to Figures 2 and 3 ■

show that the QD–MNSs exhibit super-paramagnetic behavior, which agrees with previously findings.^[17,21] Upon applying an alternating magnetic field to the QD–MNSs, the temperature was observed to rise to 52 °C within 30 min. These data can be found in the Supporting Information, (Fig: S2,S3).

In conclusion, based on the novel design of a nanostructure intended for simultaneous cancer diagnosis and treatment, QDs were immobilized on the surface of a superparamagnetic composite of polyethylene-oxide-modified PS NSs. The QD–MNSs exhibited strong fluorescence emission in the visible range of the electromagnetic spectrum. Images obtained from the first in vivo administration of QD–MNSs in live mice support further evaluation of this novel composite as an innovative, multifunctional nanodevice for biomedical applications. The unique combination of fluorescence emission and hyperthermia engineered into these NSs is anticipated to find clinical applications in early cancer diagnosis and tumor treatment.

Experimental

Qdot 800 ITK amino (PEG) QDs with an emission wavelength of 800 nm were supplied by Invitrogen Corporation (Carlsbad, CA). These QD have a CdSeTe core and a ZnS shell with a covalently attached, amine-functionalized layer of PEG. The CdSeTe/ZnS QDs were dispersed in borate buffer (8 nmol mL⁻¹). In order to assure effective surface immobilization of these QDs on the MNSs, a combined strategy of covalent coupling and electrostatic adsorption was pursued. Under physiological conditions, the positively charged amine group of the Qdot 800 ITK amino (PEG) is predicted to form electrostatically stabilized association with the electric double layer surrounding the polymer core of the MNS. Short-range, electron donor/acceptor interactions between the two surfaces are hypothesized to stabilize this association complex, which is consistent with extended DLVO (Derjaguin, Landau, Verwey, Overbeek) theory [22]. In addition, carboxyl groups resulting from auto-oxidation and partial cleavage of ethylene-oxide subunits of MNS-incorporated polysorbate [23] allow covalent coupling of the amine-functionalized QDs using conventional carbodiimide chemistry [24].

Briefly, 200 μL of a freshly prepared solution of 30 mg NHS and 10 mg EDC in 1 mL of PBS (pH 7.4) was mixed with 100 μL of a suspension containing 2 mg of MNSs and 160 pmol of QDs. The reaction mixture was incubated for 12 h at 50 °C, cooled to room temperature, and centrifuged at 12 000 rpm for 5 min. The QD–MNSs were washed three times with PBS and stored in 200 μL PBS until used.

Acknowledgements

The work performed at University of Cincinnati (UC) was supported by a grant from the UC Institute for Nanoscale Science and Technology. The TEM analyses were conducted at the Electron Microbeam Analysis Laboratory at the University of Michigan and supported by an NSF NIRT grant (EAR-0403732). Supporting Information is available online from Wiley InterScience or from the author.

- [1] D. R. Walt, *Science*. **2005**, *308*, 217.
- [2] F. Mauro, *Nat. Rev. Cancer* **2005**, *5*, 161.
- [3] X. Gao, Y. Cui, R. M. Levenson, L. W. K. Chung, S. Nie, *Nat. Biotechnol.* **2004**, *22*, 969.
- [4] B. Dubertret, P. Skourides, D. J. Norris, V. Noireaux, A. H. Brivanlou, A. Libchaber, *Science* **2002**, *298*, 1759.
- [5] X. Wu, H. Liu, J. Liu, K. N. Haley, J. A. Treadway, J. P. Larson, N. Ge, F. Peale, M. P. Bruchez, *Nat. Biotechnol.* **2003**, *21*, 41.

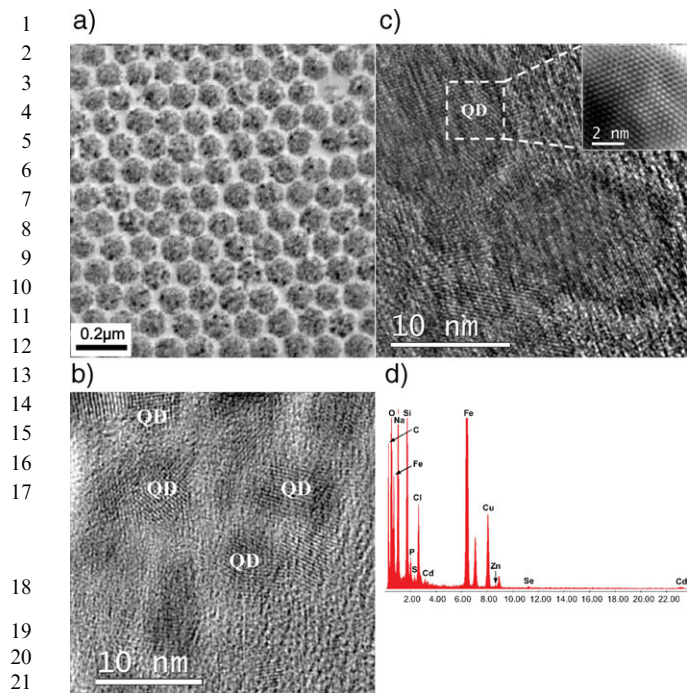


Figure 3. a) Bright-field TEM image elucidating surface structure of the QD–MNSs. b) High-resolution TEM image depicting surface properties of fabricated QD–MNSs. c) Fourier-transformed image of a randomly selected nanoparticle, which can be indexed either by hexagonal CdS or quartzite, ZnS. d) Energy dispersive X-ray (EDS) spectrum showing chemical signals of surface-associated CdSe/ZnS QDs.

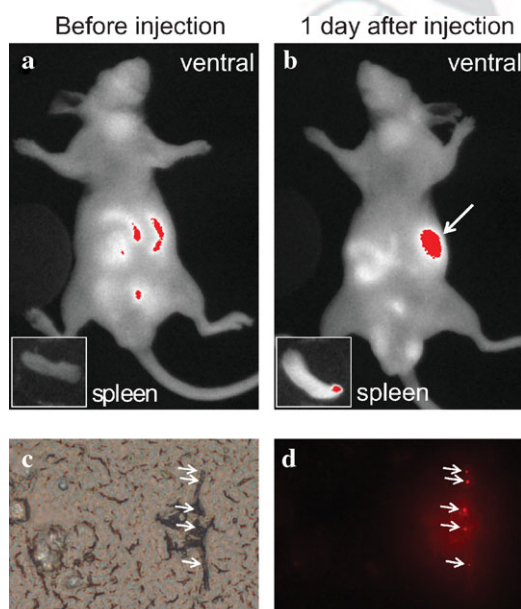


Figure 4. In vivo and ex vivo images after intravenous injection of QD–MNSs in nude mice. Red fluorescence signals indicate QD–MNS accumulation in the spleen; a) in vivo fluorescence before injection; b) in vivo fluorescence one day after injection; c) bright-field microscope image of a histological spleen section, and d) corresponding fluorescence image of the same section of tissue shown in (c).

- 1 [6] J. K. Jaiswal, H. Mattoussi, J. M. Mauro, S. M. Simon, *Nat. Biotechnol.* **2003**,
2 21, 47. 1
- 3 [7] D. R. Larson, W. R. Zipfel, R. M. Williams, S. W. Clark, M. P. Bruchez, F. W.
4 Wise, W. W. Webb, *Science* **2003**, 300, 1434. 3
- 5 [8] A. M. Derfus, W. C. W. Chan, S. N. Bhatia, *Nano Lett.* **2004**, 4, 11. 4
- 6 [9] E. B. Voura, J. K. Jaiswal, H. Mattoussi, S. M. Simon, *Nat. Med.* **2004**, 10,
7 993. 5
- 8 [10] S. Park, T. A. Taton, C. A. Mirkin, *Science* **2002**, 295, 1503. 6
- 9 [11] D. Shi, J. Lian, W. Wang, G. K. Liu, P. He, Z. Dong, L. M. Wang, R. C. Ewing,
10 *Adv. Mater.* **2006**, 18, 189. 7
- 11 [12] V. Väisänen, H. Härmä, H. Lilja, A. Bjartell, *Luminescence* **2000**, 15,
12 389. 8
- 13 [13] W. C. W. Chan, S. M. Nie, *Science* **1998**, 281, 2016. 9
- 14 [14] X. Gao, Y. Cui, R. M. Levenson, L. W. K. Chung, S. M. Nie, *Nat. Biotechnol.*
15 **2004**, 22, 969. 10
- [15] R. Hergt, S. Dutz, R. Mueller, M. Zeisberger, *J. Phys. : Condens. Matter* **2006**,
18, S2919–. 11
- [16] X. Michalet, F. F. Pinaud, L. A. Bentolila, J. M. Tsay, S. Doose, J. J. Li, G.
Sundaresan, A. M. Wu, S. S. Gambhir, S. Weiss, *Science* **2005**, 307, 538. 12
- [17] X. M. Wang, H. C. Gu, Z. Q. Yang, *J. Magn. Magn. Mater.* **2005**, 293, 334. 13
- [18] M. Babincov, V. Altanerov, C. Altaner, P. Caronic-Caronmanec, P. Babinec,
Med. Phys. **2004**, 31, 2219. 14
- [19] H. Xu, L. L. Cai, N. H. Tong, H. Gu, *J. Am. Chem. Soc.* **2006**, 128, 15582. 15
- [20] R. Weissleder, *Nat Biotech.* **2001**, 19, 316. 16
- [21] P. C. Fannin, S. W. Charles, *J. Phys. D: Appl. Phys.* **1994**, 27, 185. 17
- [22] J. A. Brant, A. E. Childress, *Environ. Eng. Sci.* **2002**, 19, 413. 18
- [23] M. Khossravi, Y. H. Kao, R. J. Mrsny, T. D. Sweeney, *Pharm. Res.* **2002**, 19,
634. 19
- [24] G. T. Hermanson, in *Bioconjugate Techniques*, Academic Press, London
1996, pp. 8, 9. 20

Q1: Please clarify throughout the article all editorial/technical requests marked by black boxes.

